

**The Optical Gravitational Lensing Experiment.
The OGLE-III Catalog of Variable Stars.
X. Enigmatic Class of Double Periodic Variables
in the Large Magellanic Cloud ***

R. Poleski¹, I. Soszyński¹, A. Udalski¹, M. K. Szymański¹,
M. Kubiak¹, G. Pietrzyński^{1,2}, Ł. Wyrzykowski³ and K. Ulaczyk¹

¹ Warsaw University Observatory, Al. Ujazdowskie 4, 00-478 Warszawa, Poland
e-mail: (rpoleski,soszynsk,udalski,msz,mk,pietrzyn,kulaczyk)@astrouw.edu.pl

² Universidad de Concepción, Departamento de Física, Casilla 160-C, Concepción, Chile

³ Institute of Astronomy, University of Cambridge, Madingley Road, Cambridge CB3
0HA, UK

e-mail: wyrzykow@ast.cam.ac.uk

Received September 15, 2010

ABSTRACT

The tenth part of the OGLE-III Catalog of Variable Stars contains 125 Double Periodic Variables (DPVs) from the Large Magellanic Cloud. DPVs are semi-detached binaries which show additional variability with a period around 33 times longer than the orbital period. The cause of this long cycle is not known and previous studies suggest it involves circumbinary matter.

We discuss the properties of the whole sample of the LMC DPVs and put more attention to particularly interesting objects which may be crucial for verifying hypothesis explaining long cycle variability. Secondary eclipses of one of the objects disappear during some orbital cycles and primary eclipses are deeper during long cycle minimum.

Key words: *Catalogs – binaries: close – Magellanic Clouds*

1. Introduction

Double Periodic Variables (DPVs) were first recognized as a separate class of variable stars by Mennickent *et al.* (2003). Their inspection of the photometry collected during the second phase of the Optical Gravitational Lensing Experiment (OGLE) revealed a group of 27 Large Magellanic Cloud (LMC) and 3 Small Magellanic Cloud (SMC) blue stars which simultaneously show two periods which ratio is close to 35.2. The light curve of the shorter period (P_1) in some instances was

*Based on observations obtained with the 1.3-m Warsaw telescope at the Las Campanas Observatory of the Carnegie Institution of Washington.

characteristic for eclipsing binaries. The longer periods (P_2) were in the interval between 140 and 960 days and the shape of the light curves was sinusoidal in most cases. It was speculated that the latter periods were caused by the precession of an elliptical disk around the blue component of the semi-detached binary. Mennickent *et al.* (2005) revealed three new DPVs in the LMC and analyzed the spectroscopic observations done for some of the systems. The multi-epoch spectroscopy of two DPVs with small amplitudes and sinusoidal light curves of the short period shows that their brightness changes are caused by the ellipsoidal variation of one of the components of the binary system. This finding was crucial for assigning short periods or twice larger values of all DPVs to orbital periods of binary systems. Mennickent *et al.* (2005) also had an impression that the longer cycle variability disappears during the main eclipse, this finding was negated later on. As a consequence, this variability should be caused by a phenomenon taking place in or near the surface of brighter component. However, any of the known types of stellar variability is in the agreement with observed features. Another important finding made by Mennickent *et al.* (2005) was a period shortening and an amplitude increase in the long period of one LMC DPV. Buchler *et al.* (2009) re-investigated MACHO project photometry for 30 DPVs selected by Mennickent *et al.* (2003) and revealed that after prewhitening with the two most prominent frequencies also a sum of these frequencies is significant[†]. No further discussion of this combination frequency is given in the literature.

Mennickent *et al.* (2008) observed spectroscopically an eclipsing DPV in the LMC. Their investigation resulted in a model which contains a binary system with the Roche lobe-filling secondary, hotter primary star with the circumprimary disk, mass transfer and mass outflow feeding the circumbinary disk. Contrary to the previous studies, it was inferred that the source of the longer cycle is in the circumbinary matter as no interference of short and long period was found. Desmet *et al.* (2010) used space mission CoRoT photometry and high-resolution ground-based spectroscopy to investigate Galactic DPV star AU Mon. CoRoT photometry was obtained during minimum of the longer cycle. Their conclusions regarding the model of the binary are consistent with previous studies of other DPVs. High quality space-based photometry allowed finding two additional periods in residual light curve. Both these periods are approximately a hundred times shorter than the orbital period of the binary. Djurašević *et al.* (2010) deepened the analysis of CoRoT photometry and added a hot spot and two bright spots to the models of the optically and geometrically thick disk. They explained the period-to-period changes in the CoRoT light curve by a variable contribution of the disk brightness. This changes cannot explain the long term cycle and Djurašević *et al.* (2010) concluded that the circumbinary matter has to be responsible for the long cycle variability. Another Galactic DPV – V393 Sco – was spectroscopically observed by Mennickent *et al.*

[†]Note that Buchler *et al.* (2009) used different frequencies designations in the text and in their Table 1.

(2010). They favor equatorial mass loss through the Lagrangian point L_3 and argue against the polar jets as a source of the longer cycle. The velocity of the mass lost through L_3 was estimated to be about 300 km/s.

Finding variability with a period of a few hundred days and amplitude of about 0.1 mag superimposed on the variability caused by a binary system with much shorter period is possible when the long-term uniformly obtained photometry is available. That is why almost the whole photometry of DPVs analyzed in the papers mentioned above came from the OGLE or the MACHO project – two microlensing surveys monitoring the LMC and the SMC. In this paper we use OGLE-III photometry to search for DPVs in the LMC. We increase the number of published stars of this type almost by a factor of four. Our search yields not only the higher number of DPVs in the LMC, which allows better statistical description of this group of stars, but also we present several objects with unexpected features. They may be crucial in understanding the cause of long term cycle, even though, we do not provide any self-consistent model explaining all observed features of the long term cycle.

In the next sections we discuss observations and the procedure of selecting DPVs. Section 4 presents the catalog itself and is followed by a discussion of properties of the whole sample as well as selected objects. We end with a summary and future prospects. To avoid confusion, we denote phases of the shorter (orbital) and longer cycle as ϕ_1 and ϕ_2 , respectively. In the case of the orbital cycle $\phi_1 = 0$ corresponds to the minimum light (primary eclipse in eclipsing systems), while for the longer cycle $\phi_2 = 0$ corresponds to the maximum light, which is more distinctive in most cases. Similarly, frequencies f_1 and f_2 are equal $1/P_1$ and $1/P_2$, respectively.

2. Observations

The OGLE-III project observed the LMC between June 2001 and May 2009 and covered around 40 square degrees. The observations were conducted with the 1.3 m Warsaw Telescope situated at Las Campanas Observatory, which is operated by Carnegie Institution of Washington. The telescope was equipped with the eight chip mosaic camera with the total dimension $8k \times 8k$ pixels. The pixel size of $15 \mu\text{m}$ gives the pixel scale of $0''.26$ and the total field of view around $35' \times 35'$. The detailed description of the instrumentation can be found in Udalski (2003). The photometry was performed using Difference Image Analysis technique (Alard and Lupton 1998, Alard 2000, Woźniak 2000) which works very well in crowded fields. Udalski *et al.* (2008a) give full description of the photometric and astrometric data reduction process. The DIA photometric uncertainties are known to be underestimated and thus were corrected using the method described by Wyrzykowski *et al.* (2009).

Typically, there are 500 photometric measurements per star obtained during OGLE-III observations. Around 90% of them were secured using I filter. The rest was taken in the V -band. For stars in the central parts of the LMC we con-

nected OGLE-III and OGLE-II photometry (Szymański 2005) obtained from 1997 to 2000. To keep the data in the same photometric system we added to the OGLE-II magnitudes the difference between median OGLE-III and OGLE-II magnitudes. In some cases with a different sampling of the short or long cycles, additional correction found manually was added. Similar procedure was carried out for objects present in two or three OGLE-III fields in the overlapping parts of adjacent fields. Our final photometry contains up to 1500 *I*- and 270 *V*-band measurements. One may find *B*-band mean magnitudes for stars in central parts of the LMC in Udalski *et al.* (2000).

3. Selection of DPVs

We have searched for characteristic period ratio in the results of the massive period search done for OGLE-III photometry of all stars observed in the LMC by the OGLE-III survey (Soszyński *et al.* 2008). More intense search was performed for stars in the region of the color–magnitude diagram where DPVs are expected ($V - I < 0.6$ mag and $V < 19$ mag; Mennickent *et al.* 2005). For these blue objects we used prewhitening with a variety of a different number of Fourier harmonics. In all cases the stars with the period ratios in a broad region around expected value of 35, even two times larger or smaller, were visually examined. Altogether 113 DPVs were selected in this way.

We suspected that our searches still may not reveal all the DPVs because automatic search for eclipsing binary periods may give spurious results (Derekas *et al.* 2007). Fourier fitting procedure with fallacious number of harmonics may also cause some artifacts in prewhitened light curve hampering searches for the additional longer period. Because of that we decided to visually inspect light curves of automatically selected eclipsing binaries candidates with periods longer than one day.[‡] 26 000 blue candidates and 7700 candidates without color information in OGLE-III data were inspected and stars showing light curves typical for DPVs phased with the orbital period were selected and studied in more detail. Additional eight stars were added to the list of DPVs. Another three DPVs were found by authors during other variability searches.

Our list of DPVs in the LMC was cross-matched with the stars found by Mennickent *et al.* (2003) and Mennickent *et al.* (2005). One of their stars was not detected by our procedure. Its designation is OGLE-LMC-DPV-114 (MACHO ID: 76.9844.110). This star does not have the *V*-band magnitude in the OGLE-III photometric maps (Udalski *et al.* 2008b) and it was not among the eclipsing binary candidates inspected visually. We decided to add it to our catalog. We note that our selection process was less efficient for stars with orbital periods shorter than one day as many artifacts appear in this period range. Also stars with exceptionally large P_2 values or ones with $P_2 \approx 1$ yr could have been overlooked.

[‡]The catalog of Magellanic Clouds eclipsing binaries with periods longer than one day is under construction by Graczyk *et al.* (in preparation).

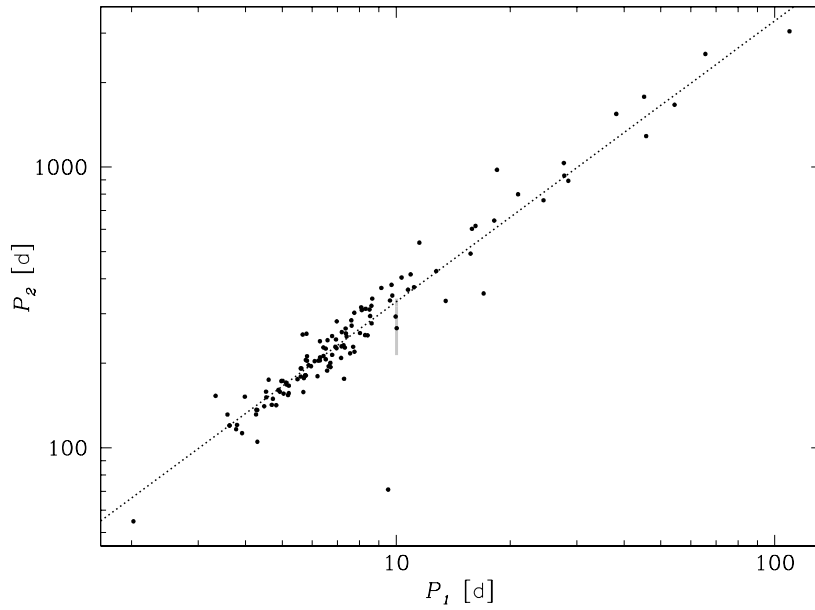


Fig. 1. Relation between the orbital and long period. Uncertainties of periods are smaller than size of points. Dotted line represents the relation $P_2 = 33.13P_1$. Gray vertical line shows the periods of OGLE-LMC-DPV-065 during the last 18 years. See Section 5.7 for discussion.

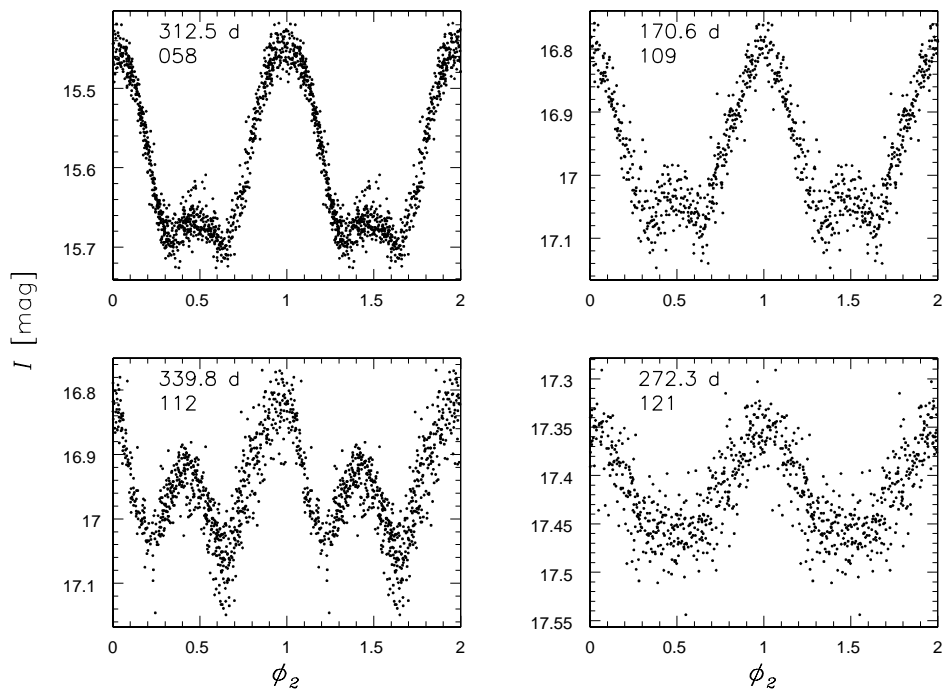


Fig. 2. Exemplary non-sinusoidal light curves of long cycles. Values of P_2 and catalog numbers in the catalog are given in each panel.

Fig. 1 shows the P_1-P_2 relation for all detected DPVs. The median value of P_2/P_1 is 33.13 and the dotted line shows this relation. The same diagram made using preliminary periods showed twelve stars with P_2 values twice smaller than the rest with similar P_1 . For these objects we multiplied P_2 by a factor of two. Fig. 2 presents four exemplary light curves showing non-sinusoidal signal or even two maxima in one cycle. They ensure us that these twelve stars do not differ significantly from other DPVs if we take P_2 twice longer than photometric period. The largest P_2 values are comparable to the time-span of OGLE-III observations so it is not sure if we observe periodic phenomenon. The values of P_1 lie in the range between 2 and 106 days.

All the periods were verified using software TATRY utilizing mhAOV method described by Schwarzenberg-Czerny (1996). All the light curves were prewhitened with case-by-case selected number of Fourier harmonics. The second periods were also checked using mhAOV method. We note that in first periodograms we see P_2 or $P_2/2$ as a dominant twice more often than P_1 or $P_1/2$.

4. Catalog

The OGLE-III catalog of DPVs in the LMC contains 125 objects and, identically as other parts of the OGLE-III Catalog of Variable Stars, is available through the OGLE Internet archive both as a user-friendly WWW interface and from the anonymous FTP site:

*http://ogle.astrouw.edu.pl/
ftp://ftp.astrouw.edu.pl/ogle/ogle3/OIII-CVS/lmc/dpv/*

The FTP site contains file *ident.dat* which successive columns contain: catalog designation in the form OGLE-LMC-DPV-XXX where XXX is consecutive number (the objects were sorted in order of increasing right ascension), two columns giving OGLE-III designation taken from Udalski *et al.* (2008b), equinox J2000.0 right ascension and declination, cross-identification with the OGLE-II and MA-CHO photometric databases and cross-identification with the extragalactic part of the General Catalog of Variable Stars (Artyukhina *et al.* 1995). File *DPV.dat* gives for each star: I and V magnitudes corresponding to the mean brightnesses of long cycle and maximum brightnesses of orbital cycle, properties of orbital variability (period and its uncertainty, epoch of the minimum light, peak-to-peak amplitude in the I -band) and properties of the longer cycle (the same as for the orbital one but with the epoch of the maximum instead of minimum light). Additional remarks for individual objects are given in the file *remarks.dat*. The subdirectory *phot/* contains multi-epoch V - and I -band OGLE photometry. Finding charts are given in the subdirectory *fcharts/*. The $60'' \times 60''$ charts are orientated with N up and E to the left.

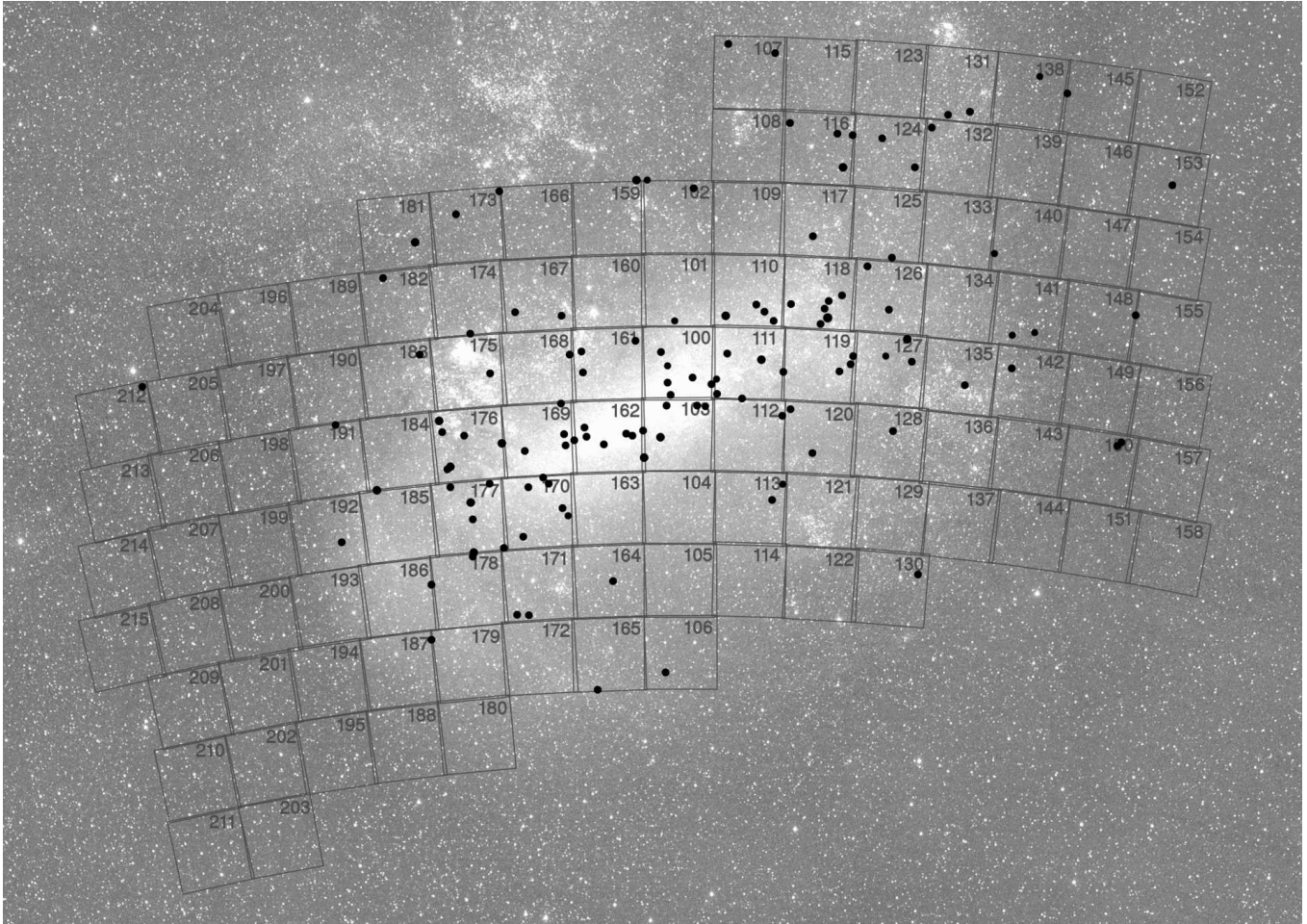


Fig. 3. Spatial distribution of DPVs in the LMC. Background squares show OGLE-III fields. The image of the LMC comes from Pojmański (1997).

Fig. 3 presents the spatial distribution of presented DPVs. Most of them are found in the LMC bar, thus we do not suspect many of these objects to lie outside the OGLE-III fields of the LMC.

5. Discussion

In this section we firstly discuss the properties of DPVs as a group and then describe in details the most interesting individual objects.

5.1. Color–Magnitude Diagram

The color–magnitude diagram (CMD) is shown in Fig. 4. For calculation of extinction-corrected $(V - I)_0$ colors and I_0 brightnesses we used Pejcha and Stanek (2009) map. Five of the reddest stars with $(V - I)_0 > 0.75$ mag show light curves at least slightly different from other DPVs and thus were marked as uncertain. One

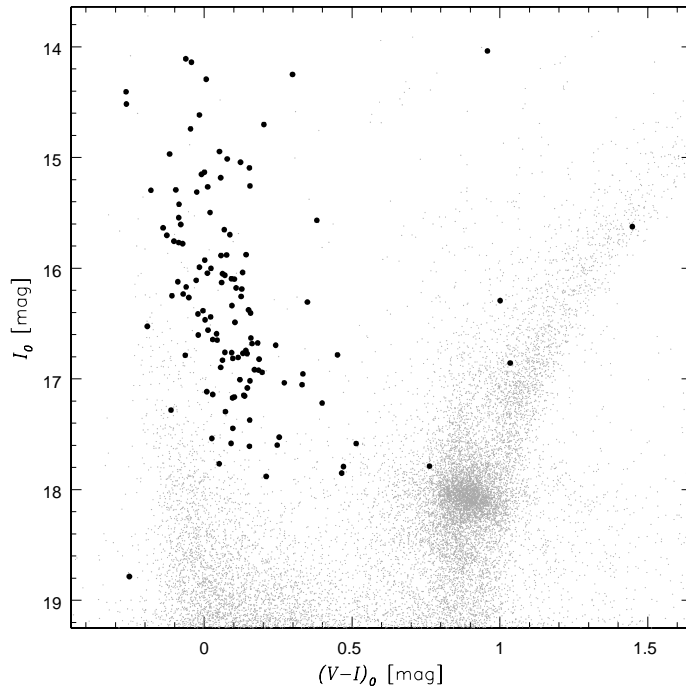


Fig. 4. Color-magnitude diagram for DPVs. Gray background shows a sample of stars from OGLE-III subfield LMC162.4 for comparison.

of them (OGLE-LMC-DPV-074) shows an interaction of the shorter and longer cycles what convinced us that both periodicities originate in the same object. It is characterized below. The short cycle light curve of the faintest DPV is not a typical light curve of binary system. This object is also marked as uncertain. All the other DPVs are in the region of CMD restricted by relations $I_0 < 17.9$ mag and $(V - I)_0 < 0.59$ mag. They are brighter than the main sequence stars with the same color what is consistent with their binary nature. Some DPVs may be overexposed in the OGLE-III images and thus not included in our catalog.

5.2. Amplitude of the Long Cycle During Minimum of the Orbital Cycle

We have visually inspected all the unfiltered light curves phased with the long and short periods to search for connections between both cycles. We did not find any such connection except for a few examples mentioned below. Mennickent *et al.* (2005) suggested that the long cycle variability disappears during the primary minimum. We do not confirm this conclusion in general case. In Fig. 5 we show two light curves with ϕ_1 limited to $(-0.1, 0.6)$ interval. The stars are the same as shown by Mennickent *et al.* (2005) in their Fig. 12. Similarly to Mennickent *et al.* (2008) we think that the suggestion of Mennickent *et al.* (2005) was an effect of the high inclination of the eclipse branches. Also small number of measurements in short ϕ_1 interval might have affected the visual impression.

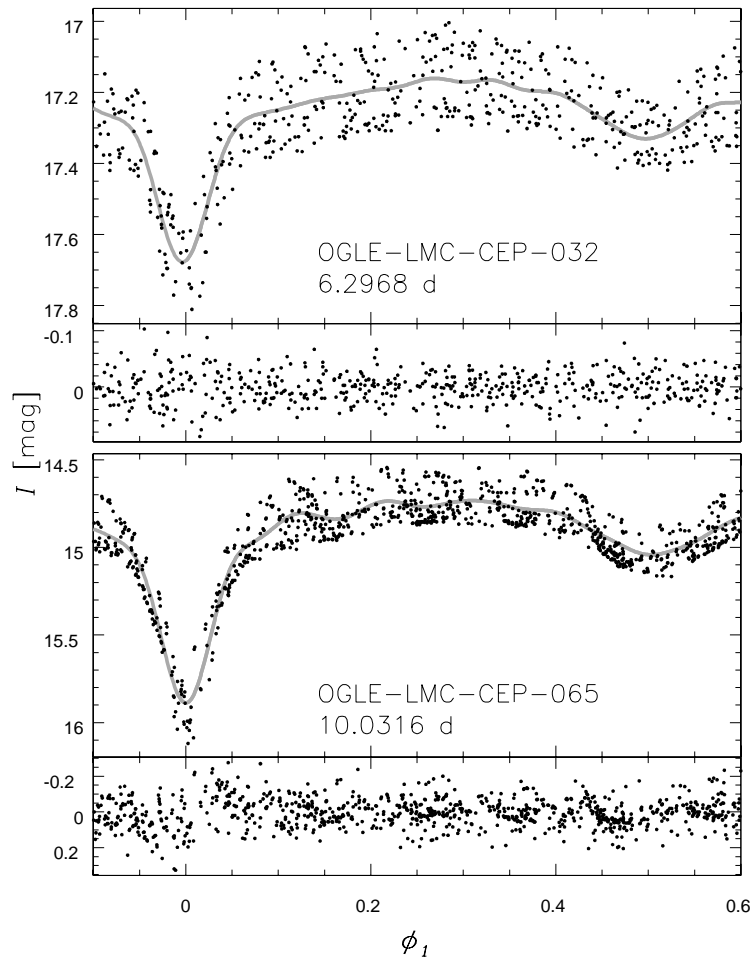


Fig. 5. Orbital light curves of two DPVs presented by Mennickent *et al.* (2005). Only phases from -0.1 to 0.6 are shown. Designations of stars and their orbital periods are given in each panel. Gray lines represent Fourier fits and residuals are given below each light curve. No definite dependence of long cycle amplitude on phase of the orbital cycle is seen.

5.3. Combination Frequencies

All the light curves were prewhitened with both P_1 and P_2 periods and periodograms were calculated for residual data. We checked if significant frequencies found during that search are linear combinations of f_1 and f_2 . Table 1 presents for each star for which we found combination frequency the period corresponding to it (column 2) and its equivalence (column 3). Altogether 36 stars are listed which is 29% of the sample. Most common are $f_1 + f_2$ combinations which are found in 30 cases.

Out of ten LMC DPVs for which Buchler *et al.* (2009) found combination frequencies we confirm five cases. They prewhitened data using half of P_1 and P_2 , we used P_1 and P_2 . The results are very similar – around 30% of DPVs show these

Table 1
Combination frequencies

ID	P_3 [day]	f_3	ID	P_3 [day]	f_3
OGLE-LMC-DPV-002	4.1640	$f_1 + f_2$	OGLE-LMC-DPV-077	6.5933	$f_1 + f_2$
OGLE-LMC-DPV-015	8.1342	$f_1 + f_2$	OGLE-LMC-DPV-078	7.0423	$f_1 + f_2$
OGLE-LMC-DPV-019	7.1568	$f_1 + f_2$	OGLE-LMC-DPV-080	7.0893	$f_1 + f_2$
OGLE-LMC-DPV-020	8.2769	$f_1 + f_2$	OGLE-LMC-DPV-083	6.4859	$f_1 + f_2$
OGLE-LMC-DPV-021	7.1819	$f_1 + f_2$	OGLE-LMC-DPV-084	15.4522	$f_1 + f_2$
OGLE-LMC-DPV-027	6.0406	$f_1 + f_2$	OGLE-LMC-DPV-088	4.4439	$2(f_1 + f_2)$
OGLE-LMC-DPV-029	5.0362	$f_1 + f_2$	OGLE-LMC-DPV-089	6.9880	$f_1 + f_2$
OGLE-LMC-DPV-034	25.3273	$f_1 - f_2$	OGLE-LMC-DPV-092	18.1226	$f_1 + f_2$
OGLE-LMC-DPV-035	7.4471	$f_1 + f_2$	OGLE-LMC-DPV-097	7.5582	$f_1 + f_2$
OGLE-LMC-DPV-038	9.5017	$f_1 + f_2$	OGLE-LMC-DPV-098	5.4605	$f_1 + f_2$
OGLE-LMC-DPV-047	5.6602	$f_1 + f_2$	OGLE-LMC-DPV-101	3.9654	$2(f_1 + f_2)$
OGLE-LMC-DPV-048	10.3202	$f_1 - f_2$	OGLE-LMC-DPV-102	5.6999	$f_1 + f_2$
OGLE-LMC-DPV-050	5.5382	$f_1 + f_2$	OGLE-LMC-DPV-105	7.3005	$f_1 + f_2$
OGLE-LMC-DPV-063	23.7287	$2(f_1 + f_2)$	OGLE-LMC-DPV-115	7.4150	$f_1 + f_2$
OGLE-LMC-DPV-064	4.6620	$f_1 + f_2$	OGLE-LMC-DPV-116	5.5946	$f_1 + f_2$
OGLE-LMC-DPV-066	9.3615	$f_1 + f_2$	OGLE-LMC-DPV-118	5.4874	$f_1 + f_2$
OGLE-LMC-DPV-067	5.5608	$f_1 + f_2$	OGLE-LMC-DPV-119	4.8723	$f_1 + f_2$
OGLE-LMC-DPV-069	6.4867	$f_1 + f_2$	OGLE-LMC-DPV-123	6.1941	$2(f_1 + f_2)$

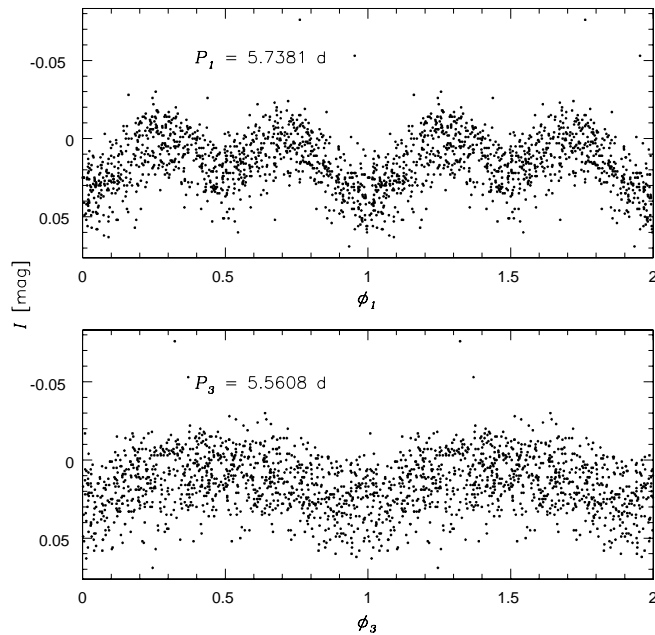


Fig. 6. Light curve of OGLE-LMC-DPV-067 prewhitened with $P_2 = 179.96$ days and phased with P_1 (upper panel) and P_3 (lower panel). P_3 is a combination periodicity.

additional frequencies. Combination frequencies may emerge after prewhitening with two frequencies if periods used are inaccurately determined or wrong number of harmonics are used. For a randomly selected DPV with a combination frequency we show the light curve after subtraction of long cycle (Fig. 6) phased with both P_1 and P_3 . The signal with a period P_3 is seen before prewhitening with P_1 what is a strong suggestion that P_3 is not an artifact.

Except for frequencies reported above we also found other which were not combinations of f_1 and f_2 . We report them in the remarks to the catalog.

5.4. OGLE-LMC-DPV-074 – Smaller Amplitude of Long Cycle During Primary Eclipse

The light curve of this object is quite different from the remaining DPVs described here. The upper panel of Fig. 7 presents the light curve of OGLE-LMC-DPV-074 folded with the orbital period. The lower panel shows data prewhitened with the orbital cycle, and still phased with the orbital period. One can easily notice that the differences between the fitted Fourier series and the actual measurements

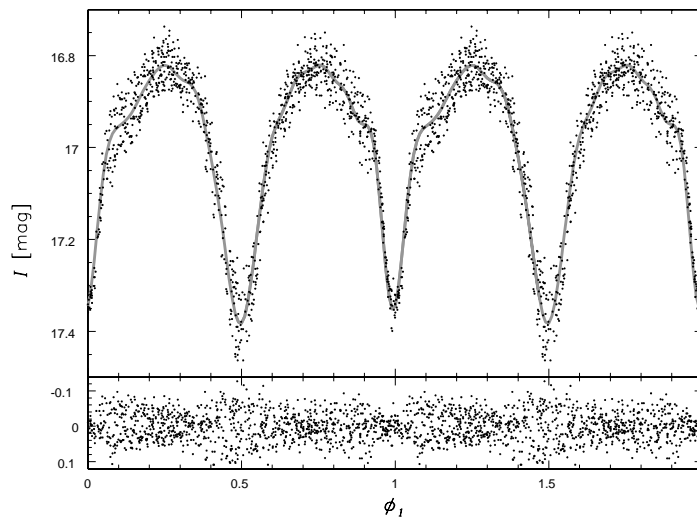


Fig. 7. Light curve of OGLE-LMC-DPV-074 ($P_1 = 38.1592$ days) with the fitted Fourier model and phased with the orbital period. *Lower panel* shows residuals. Long cycle activity weakens close to phase 0.

are much smaller close to $\phi_1 = 0$ than close to $\phi_1 = 0.5$. It seems that the amplitude of the longer cycle gets smaller close to $\phi_1 = 0$. In fact we are not sure which of the eclipses is primary and which one is secondary, because the depth of the minimum at $\phi_1 = 0.5$ changes from cycle to cycle. A similar depth of both minima suggests that temperatures of both components are similar. The orbital period of this object is very long (≈ 38.2 days) compared to other DPVs. The mean light curve is typical for semi-detached or contact binary systems, thus, we suspect the radius of the donor star is also one of the biggest among donors of known DPVs

or the total mass of the binary is smaller than for the other DPVs. We suppose the changes in brightness of the components of the binary are in the circumprimary disk or matter which left the gravitational potential of the binary through L_3 point. The smaller amplitude of the longer cycle during the eclipse near $\phi_1 = 0$ in Fig. 7 suggests that during that eclipse the donor is closer to the observer and completely hides the primary star and, at least, a substantial part of the disk. The donor does not change its surface brightness and thus, close to $\phi_1 = 0$ we see small dispersion of measurements around the fitted model. In the opposite situation, when the primary component is closer to the observer, changes in the brightness of the disk and probable matter close to L_3 point affect the brightness measured by the observer. This changes cause the observed dispersion of points seen in the light curve.

5.5. *OGLE-LMC-DPV-097 – Deeper Primary Eclipses in Long Cycle Minimum and Disappearing of Secondary Eclipses*

The light curve of this interesting DPV is shown in Fig. 8. The same symbols in both panels correspond to the same epochs of observations. The upper panel presents unfiltered data folded with the longer period and the lower one – light curve prewhitened with the longer cycle and folded with the orbital period. On the upper panel one can see four points, which are marked as crosses, clearly fainter than all the other. All of these points are close to $\phi_2 = 0.5$. The same points are shown in the lower panel and they turn out to be four out of five the faintest measurements and all of them are in the middle of the primary eclipse. The third faintest point (filled triangle) in the lower panel corresponds to the point at coordinates $\phi_2 = 0.66$ and $I = 16.50$ mag in the upper panel *i.e.*, it is also close to the minimum light of the longer cycle and is fainter than other measurements at the same phase of the longer cycle. During the primary minimum the primary star and the disk around it are hidden behind the secondary. The feature described above suggests that, at least for this particular DPV, the long cycle originates near the circumprimary disk.

The other feature seen in Fig. 8 is a disappearing of the secondary minimum of the orbital cycle. This phenomenon is seen only during the minimum light of the longer cycle. To show this feature we divided the points in the orbital phases between 0.4 and 0.6 into two groups using a horizontal line not shown in Fig. 8. The points below this line (*i.e.*, during the secondary minimum) are marked as empty squares and the ones above the line (*i.e.*, where the secondary minimum is not observed) are marked with filled circles. When we look at the distribution of these points on the upper panel we see that almost all filled circles have brightness below mean brightness of the long cycle. The empty squares are distributed almost uniformly during the long cycle, however, it seems their number is smaller near the long cycle minimum. The exact interpretation is hampered by the scatter of points which remains after prewhitening with both cycles. We tried to differently divide points between orbital phases 0.4 and 0.6 but no simple division scheme neither

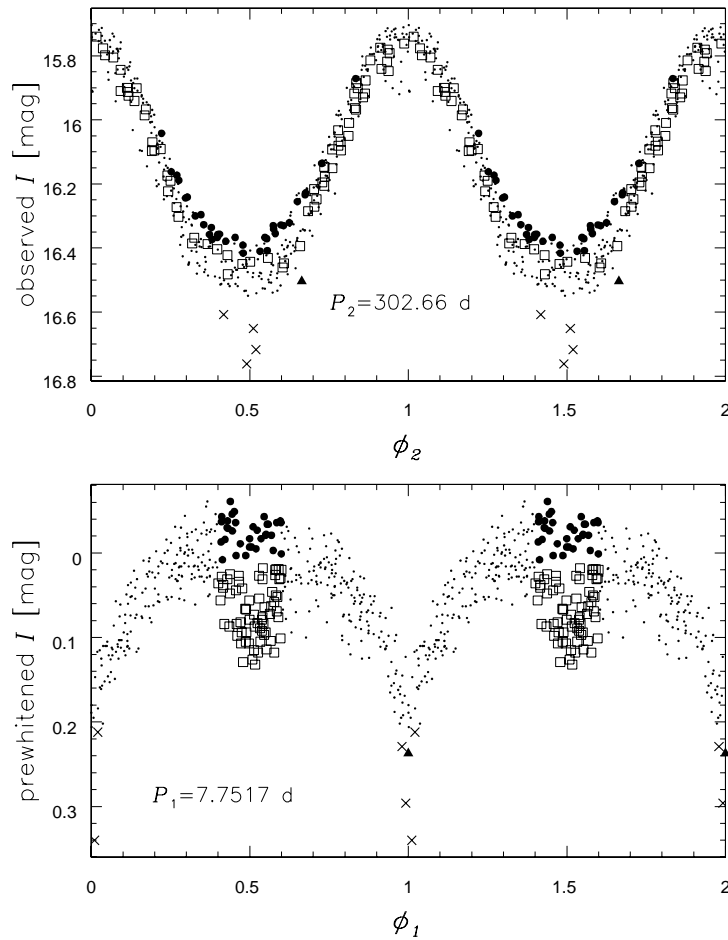


Fig. 8. Light curve of OGLE-LMC-DPV-097. *Upper panel* shows the unfiltered data phased with the longer period and *lower panel* shows prewhitened data phased with the orbital period. For each epoch the same symbols are used on both panels: empty squares are points from secondary eclipse, filled circles correspond to measurements obtained at the same phases of shorter period but when the secondary eclipse was not seen, crosses mark four the faintest measurements of the longer cycle, filled triangle – third faintest point after prewhitening and all other measurements are marked as dots.

gave better visualization nor showed additional features.

The naive explanation of disappearing of secondary eclipses may be the change of the temperature ratio of both components of the binary. The distribution of the filled circles suggests this ratio is closer to one during the minimum than during the maximum of longer cycle. However, empty squares observed during the minimum of the longer cycle contradict this interpretation.

5.6. OGLE-LMC-DPV-098 and OGLE-LMC-DPV-108 – Deeper Primary Eclipses in Long Cycle Minimum

We observe deeper primary eclipses during the long cycle minimum not only for OGLE-LMC-DPV-097. Unfortunately, in most cases the number of points fainter than the remaining measurements with similar ϕ_2 is small and thus inconclusive. The best examples of stars showing deeper primary eclipses when $\phi_2 \approx 0.5$ are OGLE-LMC-DPV-098 and OGLE-LMC-DPV-108, which light curves are shown in Fig. 9 on the left and right panels, respectively. The top panels show unfiltered light curves phased with P_2 , middle ones – light curves prewhitened with the long cycle and folded with P_1 and bottom – enlargement of the middle panel near $\phi_1 = 0$. The points outside the primary eclipses (*i.e.*, $0.04 < \phi_1 < 0.96$) are marked with dots. For a better demonstration of the effect we divided the points in the primary eclipses into two groups: ones near $\phi_2 = 0$ (gray pentagons) and ones near $\phi_2 = 0.5$ (crosses). The exact limits for crosses are $0.25 < \phi_2 < 0.75$ for OGLE-LMC-DPV-098 and $0.12 < \phi_2 < 0.88$ for OGLE-LMC-DPV-108. This means that the separation into crosses and gray pentagons is done using ϕ_2 but lower panels of Fig. 9 show that pentagons do not appear at the deepest locus of primary eclipse.

Even though the criteria for the division of points in the primary eclipse into two groups were selected manually, it is very likely that the effect described above is not a random fluctuation of observations. We note that the median uncertainties for points in the primary eclipse are 0.009 mag and 0.013 mag for OGLE-LMC-DPV-098 and OGLE-LMC-DPV-108, respectively.

5.7. OGLE-LMC-DPV-065 – Period Changes

Mennickent *et al.* (2005) called attention to the star LMC_SC6_57364 which we designated as OGLE-LMC-DPV-065. They found out that between JD 2448800 and 2450000 the long term period was 340 days, while it shortened to 270 around JD 2450500. We tried to construct $O - C$ diagram for this star using method described by Poleski (2008), however, the period changes of this object are so rapid that it is hard to reliably construct the mean light curve. In fact the light curve also changes its shape. We decided to divide OGLE photometry of this object into several chunks and use Schwarzenberg-Czerny (1996) method to measure periods separately in each chunk. Gray vertical line in Fig. 1 presents the range of P_2 values found by Mennickent *et al.* (2005) and in this study. We suspect the object may move on the $P_1 - P_2$ diagram much below the dashed line *i.e.*, where no DPVs are observed. Values of P_2 as a function of time are presented in Fig. 10 together with the linear fit to the data. The abscissa values are average epochs in each of the chunks. The fit shown was used to estimate average rate of period change which equals $dP_2/dt = -0.01724 \pm 0.00040$. It is so rapid that if dP_2/dt remains constant the longer period will be 0 around year 2040. A few other DPVs show obvious period changes with much smaller rate. Detailed investigation of the period

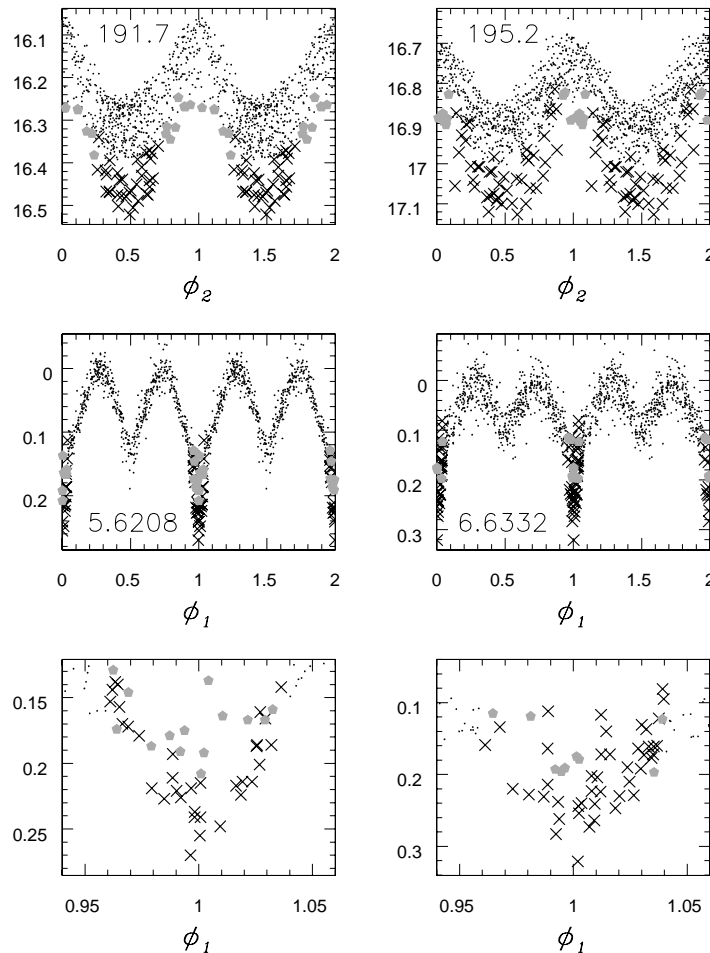


Fig. 9. Illustration of the larger amplitude of the primary eclipse during the minimum of the longer cycle for OGLE-LMC-DPV-098 (*left panels*) and OGLE-LMC-DPV-108 (*right panels*). Values of P_2 and P_1 are given in *upper* and *middle* panels, respectively. See text for description.

variability is beyond the scope of this paper.

5.8. OGLE-LMC-DPV-054 – Additional Changes in the Light Curve

We also note that OGLE-LMC-DPV-054, similarly to OGLE-LMC-DPV-065, shows rapid changes of the light curve morphology. The photometry prewhitened with P_1 is shown in Fig. 11. The upper panel shows the I -band magnitudes as a function of time and lower panels present data phased with P_2 separately for OGLE-II (left) and OGLE-III (right). Although both phased light curves show sinusoidal variability there are two episodes of certainly non periodic behavior: $2450600 < \text{HJD} < 2451350$ and since $\text{HJD} = 2454650$ up to the end of the data time-span. If the long cycle variability is caused by circumbinary matter these two episodes may be associated with variability of the rate of mass outflow. Presented

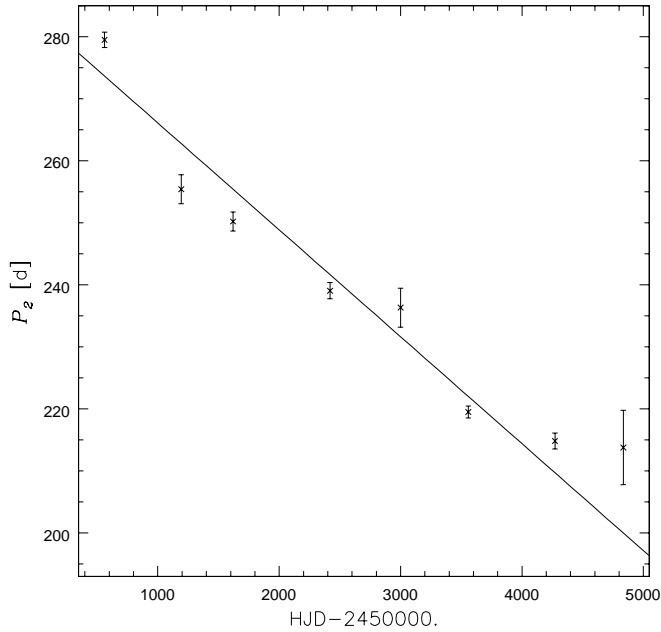


Fig. 10. Period as a function of time for OGLE-LMC-DPV-065 during OGLE-II and OGLE-III observations.

light curve does not cover the time after the second episode. Also the time-span of observations before the first episode is smaller than P_2 . We do not see distinct changes of ϕ_2 during the first episode.

6. Summary and Future Prospects

We present the OGLE-III catalog of 125 DPVs in the LMC. It contains much larger sample of these rare variable stars than known from all previous studies. The extraordinary behavior of some of the presented DPVs needs further observational efforts. Particularly interesting should be OGLE-LMC-DPV-065 with its high period change rate. Currently conducted fourth phase of the OGLE project is acquiring photometry of this object which will be analyzed in future. We also plan to observe OGLE-LMC-DPV-097 with higher cadence during the minimum of the longer cycle in order to find the shape of the secondary minimum and probably reveal the flux contribution from different components. Color information can be obtained from the archival photometry of MACHO and EROS projects each of which simultaneously observed in two different bands. Color changes of OGLE-LMC-DPV-054 during its erratic fluctuations may be very interesting. Even without this additional observations our findings should be useful for verification of hypothesis describing cause of long period variability.

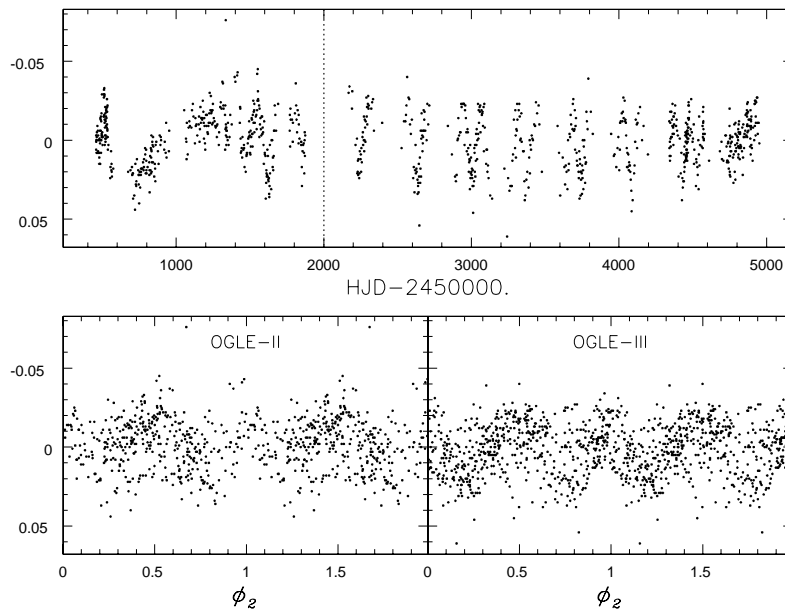


Fig. 11. Light curve of OGLE-LMC-DPV-054 prewhitened with $P_1 = 5.79598$ days. *Upper panel* shows photometric data without folding. *Lower panels* show OGLE-II (HJD < 2452000) and OGLE-III (HJD > 2452000) photometry folded with $P_2 = 254.7$ days.

Acknowledgements. Authors are grateful Prof. W. Dziembowski for fruitful discussions and R. Mennickent for reading the manuscript. We thank Z. Kołaczowski, A. Schwarzenberg-Czerny and J. Skowron for providing the software used in this study.

The research leading to these results has received funding from the European Research Council under the European Community’s Seventh Framework Programme (FP7/2007-2013)/ERC grant agreement no. 246678. RP is supported by the Foundation for Polish Science through the Start Program. This work was also supported by the MNiSW grant NN203293533 to IS. The massive period search was performed at the Interdisciplinary Centre for Mathematical and Computational Modeling of Warsaw University (ICM UW), project no. G32-3. We are grateful to Dr. M. Cytowski for helping us in this analysis.

REFERENCES

- Alard, C. 2000, *A&AS*, **144**, 363.
 Alard, C. and Lupton, R.H. 1998, *ApJ*, **503**, 325.
 Artyukhina, N.M., *et al.* 1995, “General Catalogue of Variable Stars”, 4rd ed., vol.V. Extragalactic Variable Stars, “Kosmosinform”, Moscow.
 Buchler, J.R., Wood, P.R., and Wilson, R.E. 2009, *ApJ*, **703**, 1565.
 Derekas, A., Kiss, L.L., and Bedding, T.R. 2007, *ApJ*, **663**, 249.
 Desmet, M., *et al.* 2010, *MNRAS*, **401**, 418.
 Djurašević, G., Latković, O., Vince, I., and Češki, A. 2010, *MNRAS*, in press.

- Mennickent, R.E., Pietrzyński, G., Díaz, M., and Gieren, W. 2003, *A&A*, **399**, L47.
- Mennickent, R.E., Cidale, L., Díaz, M., Pietrzyński, G., Gieren, W., and Sabogal, B. 2005, *MNRAS*, **357**, 1219.
- Mennickent, R.E., Kołaczkowski, Z., Michalska, G., Pietrzyński, G., Gallardo, R., Cidale, L., Granada, A., and Gieren, W. 2008, *MNRAS*, **389**, 1605.
- Mennickent, R.E., Kołaczkowski, Z., Graczyk, D., and Ojeda, J. 2010, *MNRAS*, **405**, 1947.
- Pejcha, O., and Stanek, K.Z. 2009, *ApJ*, **704**, 1730.
- Pojmański, G. 1997, *Acta Astron.*, **47**, 467.
- Poleski, R. 2008, *Acta Astron.*, **58**, 313.
- Schwarzenberg-Czerny, A. 1996, *ApJ*, **460**, L107.
- Soszyński, I., Poleski, R., Udalski, A., Szymański, M.K., Kubiak, M., Pietrzyński, G., Wyrzykowski, Ł., Szewczyk, O., and Ulaczyk, K. 2008, *Acta Astron.*, **58**, 163.
- Szymański, M.K. 2005, *Acta Astron.*, **55**, 43.
- Udalski, A. 2003, *Acta Astron.*, **53**, 291.
- Udalski, A., Szymański, M., Soszyński, I., and Poleski, R. 2008a, *Acta Astron.*, **58**, 69.
- Udalski, A., Szymański, M., Soszyński, I., Kubiak, M., Pietrzyński, G., Wyrzykowski, Ł., Szewczyk, O., Ulaczyk, K., and Poleski, R. 2008b, *Acta Astron.*, **58**, 89.
- Woźniak, P.R. 2000, *Acta Astron.*, **50**, 421.
- Wyrzykowski, Ł. *et al.* 2009, *MNRAS*, **397**, 1228.